THERMAL BUCKLING OF CONTINUOUOSLY WELDED RAILWAY TRACKS

Dimitrios S. Sophianopoulos, PhD
Associate Professor
Department of Civil Engineering, University of Thessaly
Volos, Greece
E-mail: dimsof@civ.uth.gr, dimsoph@otenet.gr

Jamil – Sotirios Kandalaft, MSc
Department of Civil Engineering Educators, School of Pedagogical and Technological Education, Athens, Greece
E-mail: j.swt.kandalaft@hotmail.gr

1. ABSTRACT

In this work, we offer an approximate numerical procedure for solving the problem of static out-of-plane thermal buckling of continuously welder railway tracks (CWRs). Initially, a brief overview of the underlying theory is presented, a well-accepted buckling model is adopted and the corresponding equilibrium equation is formulated in dimensionless form. Considering all relevant boundary and continuity conditions, the resulting equation is solved numerically, based on element-free Galerkin methods and adopting a 4^{th} order polynomial approximation for the postbuckling CWR shape. Utilizing advanced symbolic and algebraic manipulations, we reach to a rather easily applicable iterative procedure, which may lead to acceptable solutions in terms of critical points and equilibrium paths. A numerical application based on experimental evaluation and/or field observations shows very good accuracy, indicating of the validity of the proposed methodology.

2. INTRODUCTION

In a conventional track, the ends of the rail are joined together mechanically with a gap between, in order to allow thermal expansions in summer. Consequently, a structural weakening of the track is inevitable, following to an increase of the track maintenance cost and power consumption of the running train. These drawbacks became more serious with the introduction of modern high-speed trains.
Hence, over the past three decades significant research work was performed, with goals the improvement of ride quality, the increase of rail and rolling stock fatigue life and reduction of cost. These were the principle motivation to changing to Continuously Welded Tracks (CWRs), which differ from the jointed rail track in that rails are welded together in lengths as long as several kilometres. However, with the elimination of the joints, the constrained thermal expansion and contraction-induced compressive and tensile forces created the possibility of track buckling in the summer and tensile pull-apart failures in the winter often

causing catastrophic derailments. For this reason, substantial research has been conducted to address the CWR safety and performance through the development of analytical models [1-3], test investigations, parameter characterization studies, measurement technique development, and improvement in track maintenance practices. One of the major goals of this research aimed in understanding and controlling failure modes caused by thermal loads in the rails. Two of these modes, greatly influencing the safety of vehicle operations include the following: (a) loss of lateral stability (track buckling, track shift, and radial breathing) and (b) rail pull apart (rail break under high tensile forces).
Based on a typical CWR structure, as depicted in Figure 1, the most important buckling parameters, to be discussed in detail in later sections, are the tie-ballast resistance, the rail fastener longitudinal and torsional resistance and CWR neutral temperature (i.e. that temperature at which the net longitudinal force in the rails is zero).

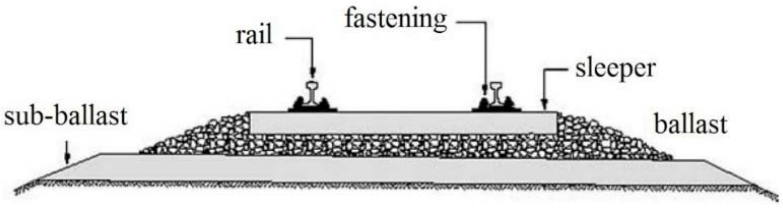

Fig. 1: Typical track structure

In the present work, we focus on investigating the static out-of-plane (lateral) thermal buckling of CWRs, and presenting an approximate technique for solving the foregoing problem. After a brief discussion of the underlying theory, the equilibrium equations are derived, using large deflection stability analysis and a well-posed model. Thereafter, adopting flat Galerkin schemes, the equations at hand are solved numerically. An indicative example is finally presented, based on experimental evaluation and/or field observations, showing adequate accuracy and efficiency, a fact indicating that the proposed method can be used for structural design purposes.

3. CWR BUCKLING THEORY

3.1 Buckling mechanism

We consider a long straight CWR track, shown in Figure 2, having a small initial sinusoidal type misalignment described by an amplitude δ_0 and a wavelength $2L_0$. With increase in rail temperature, the compressive force P will also increase, producing some growth in the initial misalignment.

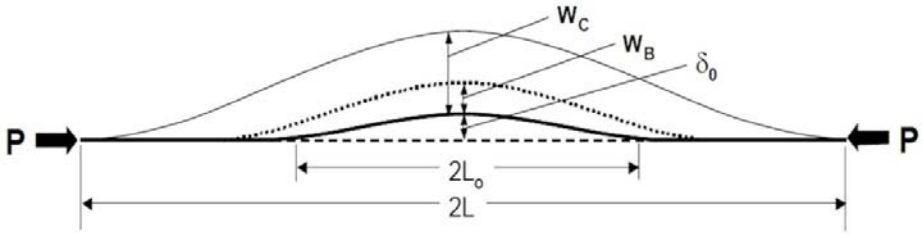

Fig. 2: Pre- and Postbuckling Track Configurations

Experiments as well as filed observations have revealed that as temperature (and the corresponding rail force) increase to a certain maximum (critical) level, the initial misalignment will also increase to an amplitude of w_B, which is in fact an unstable equilibrium state. At his state, the track may buckle out suddenly (in a snap-through manner) into a new lateral position, w_C, spanning a length of 2L. The corresponding possible equilibria are shown in Figure 3, where two distinct temperature values, namely ΔTB_{max} (bifurcation temperature) and ΔTB_{min} are present, in between which multiple equilibrium positions can exist.

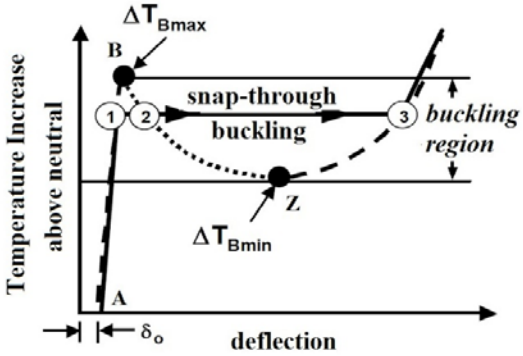

Fig. 3: Buckling Response Curve

From point A to point B we have stability (fundamental path), as well as from Z to infinite deflections (remote unacceptable configurations). Branch BZ is unstable, leading to a typical snap-through situation. Hence, the range between ΔTB_{min} and ΔTB_{max} represents the buckling regime of CWR tracks. Whereas the track will buckle at ΔTB_{max} with no external energy, it can also lose stability at ΔTB_{min} if sufficient external energy is provided to the track. Below ΔTB_{min} the system is globally stable.

3.2 Drop of force – Buckle influence zone

A feature of the buckling mechanism described above is the accompanying rail force drop (energy release) in the buckled zone, compared with that of the prebuckling force value. This is due to the large lateral displacement contributing to the rail extension that releases some of the compressive load. Thus, the rail force distribution in the buckled and adjacent zones is significantly altered, as depicted in Figure 4, resulting also to the alternation of the CWR neutral temperature after the buckling incident.

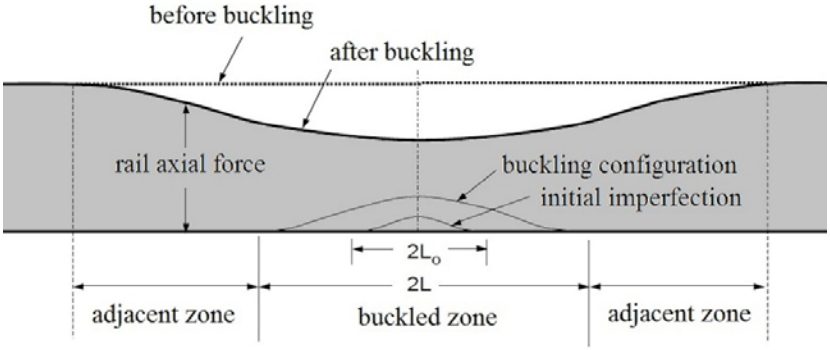

Fig 4: Rail Force Distribution after Buckling

3.3 Track model

Almost all deterministic buckling theories [4] for CWR are based on the mechanistic track model given in Figure 5. The buckling force is the combined compressive load the two rails, which depends on the rail cross-sectional area and the temperature rise. The lateral resistance generated between the ties and the ballast, as well as the longitudinal and torsional resistances generated in the rail fasteners, offer the resistive forces to the buckling force.

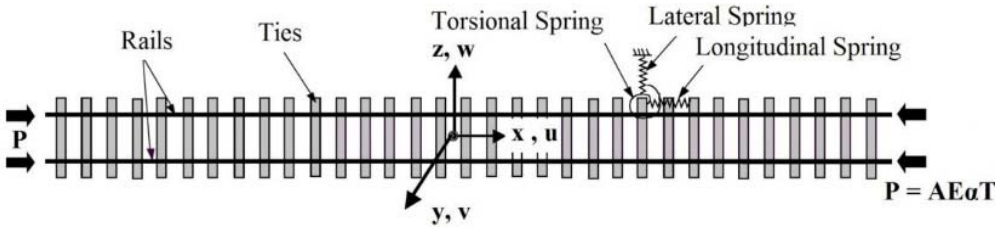

Fig 5: Track Model

The lateral resistance depends on nonlinear tie-ballast spring characteristic because the tie displaces laterally through the ballast. The longitudinal resistance depends on longitudinal spring characteristic of the rail/tie/fastener/ballast. The rail-to-tie fastenings also offer rotational rigidity (modeled by torsional springs), which reacts against the rail's tendency to rotate during the buckling deformations.

4. DIFFERENTIAL EQUATION FORMULATION

After assuming that misalignment is approximated according to the expression

$$w_0(x) = \delta_0 \left[1 - 2\left(\frac{x}{L_0}\right)^2 + \left(\frac{x}{L_0}\right)^4\right] \quad (1)$$

and accounting for the geometry and sign convention – coordinate system of Figure 6, and the chosen model, we can now proceed with the formulation of the equilibrium equations.
For the buckled zone, i.e. for $-L \le x \le L$, the differential equation of equilibrium can be written as

$$EI_{zz}\frac{d^4w(x)}{dx^4} + (\overline{P} - \tau_0)\frac{d^2w(x)}{dx^2} + \overline{P}\frac{d^2w_0(x)}{dx^2} + F(w(x)) = 0 \quad (2)$$

where EI_{zz} is the bending resistance of both rails, $\overline{P}$ the thermal compressive force and $F(w(x))$ is the distribution function of the lateral resistance, which here is considered of the following exponential form:

$$F(w) = F_L + (F_P - F_L)e^w\,,\ F(0) = F_P\ ,\ \lim_{w\to\infty} F(w) = F_L \quad (3)$$

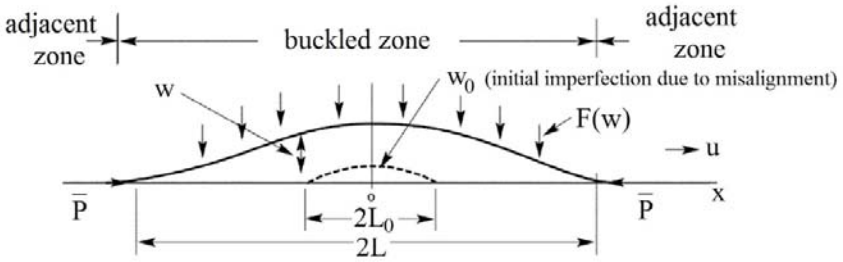

Fig 6: Geometry and Sign Convention

Additionally, τ_0 is the linear torsional resistance per unit track length.
In the adjacent zones,$|x| > L$, the longitudinal resistance is considered proportional to the relevant deformation U, so one may write

$$U'' - \rho^2 U = 0 \quad (4)$$

In the above equation, $\rho^2 = \frac{k_f}{EA}$, where k_f is the longitudinal stiffness and EA is the axial stiffness of both rails and the prime denotes differentiation with respect to x.
The solution of eq. (4) should be bounded for very large values of x, and hence we can easily find that this equation drops one order and becomes of the form

$$U' + \rho U = 0 \quad (5)$$

Equations (2) and (5) are strongly coupled through the so-called compatibility conditions (continuity of longitudinal displacements), given by

$$U(L) = -\frac{\bar{P}L}{AE} - X - a\Delta TL \,, U'(L) = -\frac{\bar{P}L}{AE} + \alpha\Delta T \quad (6a,b)$$

where, as a product of cumbersome manipulation and solving with respect to $\bar{P}$

$$X = \frac{1}{2}\int_0^L w'(x)^2\,dx - \frac{12\delta_0}{L_0^4}\int_0^L x^2 w(x)dx + \frac{4\delta_0}{L_0^2}\int_0^L w(x)dx \quad (7)$$

Introducing the following dimensionless and other simplification parameters

$$\chi = \frac{x}{L} \,, \beta(\chi) = \frac{w(x)}{L} \,, \sigma = \frac{\delta_0}{L_0} \,, \gamma = \frac{L_0}{L} \,, \xi = \frac{\tau_0}{EA} \,, \bar{\rho}^2 = \frac{k_f L^2}{EA} \,, p_1 = \frac{L}{EA}F_L \,, p_2 = \frac{L}{EA}F_P, \lambda_z^2 = \frac{A}{I_z}L^2 \text{ for each track, } \alpha \text{ the thermal expanion coeffient of steel} \quad (8)$$

Combining all the above, we reach to a strongly nonlinear integro-differential equation governing the problem in dimensionless form:

$$\frac{2}{\lambda_z^2}\beta''''(\chi) + (\alpha T - S - \xi)\beta''(\chi) + (\alpha T - S)\left(\frac{12\sigma}{\gamma^3}\chi^2 - \frac{4\sigma}{\gamma}\right) + p_1 + (p_2 - p_1)\varepsilon^{\beta(\chi)} = 0 \quad (9)$$

in which

$$S = \frac{\frac{1}{2}\int_0^1 \beta'^2(\chi)dx - \frac{12\sigma}{\gamma^3}\int_0^1 \chi^2\beta(\chi)dx + \frac{4\sigma}{\gamma}\int_0^1 \beta(\chi)dx}{1+\bar{\rho}}\bar{\rho} \quad (10)$$

Due to the profound symmetry of the problem, without any loss of generality, $\beta(\chi)$ is restricted between 0 and 1, and hence eq. (9) is associated to the following conditions:

$$\beta(1) = \beta''(1) = 0 \,, \beta'(0) = 0 \,, \overset{T=0}{\widetilde{\beta(0)}} = \sigma\gamma \quad (11\alpha\text{-}\delta)$$

5. PROPOSED NUMERICAL SCHEME

We employ in what follows a numerical scheme based on the flat Galerkin methods [5], adopting a basis function for $\beta(\chi)$ of a 4th order polynomial form, which satisfies eq. (9) and conditions (11). Imposing the three first of these conditions, the basis function yields

$$\beta(\chi) = A_4\chi^4 + \frac{1}{2}(A_0 - 5A_4)\chi^3 - \frac{3}{2}(A_0 - A_4)\chi^2 + A_0 \quad (12)$$

Substituting the above expression in eq. (9) and imposing the last of conditions (11), after symbolic computations in Mathematica [6], we reach to a 3rd order polynomial equation with respect to A_4, the coefficients of which are lengthy expression of the parameters involved, not given here for brevity. It should be noted that this equation possesses always one real root, and perhaps three real roots.
The proposed scheme consists of the following steps.

- Computation of the real roots of $f(A_4) = 0$.
- Insertion in eq. (9) of a non-zero value of T and based on the outcome of the previous step numerical solution with respect to A_0 for χ=0, which in fact is the magnitude of the dimensionless deflection in the middle for this value of T. It is possible that more than

one distinct values for A_0 will appear; these will be later qualitatively appraised, in the sense of producing structurally acceptable configurations.

- Plotting the A_0/T curves and eliminating inadmissible solutions.

6. DISCUSSION – NUMERICAL EXAMPLE

The substantial difficulty of the method lies in the correct choice of the order of magnitude for the length 2L of the buckled zone. This is so, since all dimensionalizations are based on its value. However, given that rail profiles are quite slender, especially out-of-plane, one may initially estimate L by adopting a large slenderness λ_z, together with the requirement L to be multiple of L_0. Hence, having selected the rail profile, may lead to an acceptable estimation of L. If during the process, and for small values of T, $f(A_4) = 0$ has three real roots, then L is increased gradually, until only one root is reached. If again this increase does not lead to this goal, L is gradually decreased and so on. The whole procedure can be easily programmed until the value of L is appropriately estimated.

Additionally, there exist admissible starting and ending points for the values of the initial misalignment as well as the expected length of the buckled zone. Evidently, from field observations in the US and Australia, it turned out that (in cm): $250 \leq 2L_0 \leq 1250$, $1220 \leq 2L \leq 2450$ and $1.30 \leq \delta_0 \leq 8.00$.

For the numerical example that follows the choice of the aforementioned values was rather conservative: $2L_0 = 550$ cm, $2L = 1600$ cm and $\delta_0 = 4{,}50$ cm. Furthermore, the most popular rail section in Europe was used, namely 60E1 Vignole (flat-bottomed, equivalent to UIC 60 profile), fully consolidated ballast, concrete ties and Pantrol fasteners. These choices lead to the following values of the various parameters involved [7]: k_f = 2,812 kN/cm^2 , τ_0 = 44,48 kN, I_{zz} = 1024,6 cm^4, A = 153,4 cm^2, F_P = 0,53574 kN/cm, F_L=0,17858 kN/cm. Similar experimental values (not of geometry), adequately correlated, were reported in [8] and [9].

The proposed technique started giving one real root for A_4 at approximately 2L = 1720 cm, without any computational difficulties or delays. This root was found equal to 1,32244, and based on it the equilibrium path was evaluated iteratively. Of course, for every new value of L, all dimensionless parameters were re – computed at each step. The method yielded quite satisfactory results, since the equilibria, given in Figure 7, strongly resemble the theoretical ones (see Fig. 3) with ΔTmin = 28^0 C and ΔTmax = 45^0 C (gross values).

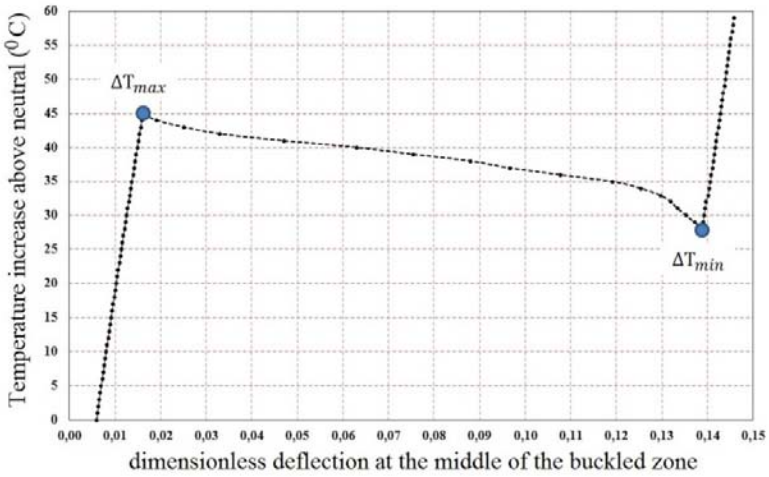

Fig 7: Equilibrium paths of the exemplary numerical application

This result is a strong indication of the validity of the proposed approximate technique. The work is ongoing, and it will eventually produce a software package for structural design of CWR tracks.

7. CONCLUSIONS

The most important conclusion of this work are:

1. The lateral (out-of-plane) thermal buckling problem of CWR tracks is multi-parametric, strongly nonlinear and profoundly difficult to deal with.
2. The proposed approximate numerical procedure seems robust, stable, with a strong theoretical background and easy to handle; it may produce reliable results, based on well-accepted parameter values.
3. Ongoing work, aiming at more sophisticated modeling and programming, could serve as a valuable tool for structural design purposes.

8. REFERENCES

[1] KERR, A.D. "Analysis of Thermal Track Buckling in the Lateral Plane", *Acta Mechanica*, Vol. 30, No. 1, 1978, pp. 17-50.

[2] LIM, N.-H., PARK, N.-H., KANG, Y.-J. "Stability of continuous welded rail track", *Computers & Structures*, Vol. 81, Nos. 22-23, 2003, pp. 2219-2236.

[3] LIM, N.-H., PARK, N.-H., KANG, Y.-J. "Parametric Study on Stability of Continuous Welded Rail Track – Ballast Resistance and Track Irregularity", *International Journal of Steel Structures*, Vol. 8, 2008, pp. 171-181.

[4] SAMAVEDAM, G. "Theory of CWR Track Stability", *ERRI report D202.RP3,* Utrecht, February 1995.

[5] FLETCHER, C.A.J. "Computational Galerkin Methods", *Springer*, 2012.

[6] DUBIN, D. "Numerical and Analytical Methods for Scientists and Engineers, Using Mathemetica", *Wiley-Interscience*, 2003.

[7] U.S. DEPARTMENT OF TRANSPORTATION, FEDERAL RAILROAD ADMINISTRATION "Track Buckling Prevention: Theory, Safety Concepts, and Applications", *Final Report DOT/FRA/OED-13/16*, March 2013.

[8] KISH, A., SAMAVEDAM, G. "Analysis of Thermal Buckling Test on United States Railroads", *DOT/FRA/ORD-82/45*, 1982.

[9] SAMAVEDAM, G., KISH. A. "Track Lateral Shift Model and Test Validation", *DOT/VNTSC/FRA Report,* 2002.

ΘΕΡΜΙΚΟΣ ΛΥΓΙΣΜΟΣ ΣΥΝΕΧΩΣ ΣΥΓΚΟΛΛΗΜΕΝΩΝ ΣΙΔΗΡΟΤΡΟΧΙΩΝ

Δρ. Δημήτριος Σ. Σοφιανόπουλος
Αναπληρωτής Καθηγητής
Τμήμα Πολιτικών Μηχανικών, Πανεπιστήμιο Θεσσαλίας
38334 Βόλος, Ελλάς
e-mail: dimsof@civ.uth.gr, dimsoph@otenet.gr

Τζαμίλ – Σωτήριος Κανταλάφτ, MSc
Ανώτατη Σχολή Παιδαγωγικής και Τεχνολογικής Εκπαίδευσης
Τμήμα Εκπαιδευτικών Πολιτικών Μηχανικών
14121 Ηράκλειο Αττικής, Ελλάς
e-mail: j.swt.kandalaft@hotmail.gr

ΠΕΡΙΛΗΨΗ

Στην παρούσα εργασία προσφέρεται μια προσεγγιστική αριθμητική μέθοδος για την επίλυση του προβλήματος θερμικού εκτός επιπέδου («πλευρικού») λυγισμού συνεχώς συγκολλημένων σιδηροτροχιών. Αρχικά παρατίθεται μια συνοπτική αναφορά της όλης θεωρίας, και κατόπι υιοθετείται ένα ευρέως αποδεκτό μηχανικό προσομοίωμα. Με βάση αυτό, μορφοποιούνται οι εξισώσεις ισορροπίας σε αδιάστατη μορφή.
Λαμβάνοντας υπ' όψη όλες τις συνοριακές συνθήκες και τις συνθήκες συμβατότητας γενικευμένων παραμορφώσεων, οι εν λόγω εξισώσεις επιλύονται αριθμητικά με βάση τη κατά τεκμήριο συμβατική μέθοδο Galerkin. Η μεταλυγισμική παραμόρφωση της τροχιάς θεωρείται μορφής πολυώνυμου $4^{ου}$ βαθμού, και κάνοντας χρήση προχωρημένων συμβολικών μαθηματικών υπολογισμών οδηγούμαστε σε μια επαναληπτική διαδικασία, εύκολα εφαρμόσιμη και εντασσόμενη σε λογισμικό. Αυτή οδηγεί σε αποδεκτές λύσεις βασισμένες σε πειραματικά αποτελέσματα και επί τόπου παρατηρήσεις, με ικανοποιητική ακρίβεια και προοπτικές για περαιτέρω έρευνα και εξέλιξη, με σκοπό το δομοστατικό σχεδιασμό.